

On the interface friction in direct shear test

S.H. Liu ^{a,*}, De'an Sun ^b, Hajime Matsuoka ^c

^a College of Water Conservancy and Hydropower Engineering, Hohai University, Xikang Road 1, Nanjing 210098, PR China

^b Department of Civil, Surveying and Engineering, University of Newcastle, NSW 2308, Australia

^c Department of Civil Engineering, Nagoya Institute of Technology, Nagoya 466-8555, Japan

Received 7 December 2004; received in revised form 1 April 2005; accepted 19 May 2005

Available online 18 July 2005

Abstract

Distinct element simulations for the direct shear box tests on a dense and a loose 2D sample of a mixture of binary diameter cylinders were performed. Special attention is focused on the friction between the internal surface of the shear box and the sample. In the conventional direct shear test, where the up/downward movement of the upper shear box is restrained and the lower shear box moves horizontally, the frictional force that acts on the sample at the internal surface of the upper shear box is downward for the dense sample and upward for the loose sample, causing the real shear strength to be larger for the dense sample and smaller for the loose sample than the one calculated from the externally applied normal force. Two possible improvements for the conventional direct shear test to reduce the frictional force of the shear box are introduced: one is free of the upper shear box vertically by adding the low friction Teflon rods and a platen between the upper shear box and the bearing ring that measures the shear force; the other is to pull the upper shear box with a flexible rope or wire. The distinct element method simulation and the experimental results show that both these two improvements can reduce the influences of the interface frictional force on the shear strengths.

© 2005 Elsevier Ltd. All rights reserved.

Keywords: Direct shear test; Distinct element method; Friction; Shear strength; Improvement

1. Introduction

The direct shear test (DST) is very popular for the laboratory testing of soils owing to its simplicity. The conventional direct shear test apparatus [1,2], as shown in Fig. 1, has both an upper and a lower shear boxes, and the sample is sheared along the plane between them by pushing the lower shear box horizontally with a normal (vertical) load applied to it. The shear force is measured with a bearing ring or a load cell that is attached to the upper shear box. A frictional force is generated at the attachment point when the upper shear box tends to move up/downward due to the volume change of the

sheared sample (dilation or contraction). Sometimes, to prevent the tilting of the upper shear box during the shearing process, a clasp is set on the opposite of the attachment point. The frictional force at the attachment point and the clasp restrain the up/downward movement of the upper shear box. Consequently, the frictional force between the interface of the upper shear box and the sample is generated due to the volume change of the sheared sample. Owing to the influence of this interface friction, the applied normal stress is generally lower for dilative specimens (like coarse granular soils) but higher for contractive ones than the true values on the shear plane (e.g. [3,4]). In this paper, distinct element simulations of the direct shear test are performed to better understand these phenomena, since they can provide microscopic information that is difficult to obtain experimentally, such as particle displacements and particle/particle contact force network. Two different initial

* Corresponding author. Tel.: +86 25 83786727; fax: +86 25 83731332.

E-mail addresses: sihong_hhu@yahoo.com.cn, sihongliu@hhu.edu.cn (S.H. Liu).

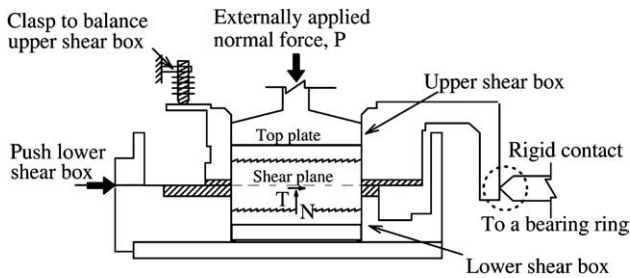


Fig. 1. Schematic of conventional direct shear test device [2].

sample densities are considered in the present work, a dense sample and a loose sample, in order to simulate the dilative specimen and the contractive specimen. Two possible improvements for the conventional direct shear test apparatus to reduce the interface frictional force of the shear box are then introduced and the distinct element simulations for these two improved direct shear box tests are also presented.

2. Discrete modeling of conventional direct shear test

2.1. Distinct element method

Laboratory experiments are usually incapable of providing insight into the microscopic characteristics of granular materials. The distinct element method (DEM), pioneered by Cundall (1971) [5] and Cundall and Strack (1979) [6], is a numerical technique that keeps track of the motion of individual particles and updates any contact with neighboring elements by using a constitutive contact law. It provides a valuable tool to obtain quantitative information of all microscopic features of an assembly of particles. In two dimensions each particle has three degrees-of-freedom (two translations and one rotation). Each particle can be in contact with neighboring particles or boundaries. In the present work, the DEM program GRADIA [7] is used. The particles in GRADIA are circular; their mechanical interaction is characterized using the so-called soft contact

approach. In this approach, although the particles are assumed to be rigid for purposes of shape definition, elastic deformation is allowed to take place at the contacts. The constitutive contact law employed in GRADIA is shown in Fig. 2(a). It consists of two parts: (1) a stiffness model providing a linear elastic relation between contact force and contact relative displacement in normal and shear directions; (2) a slip model enforcing a relation of Coulomb's type between shear and normal contact forces. Due to the dynamic formation of the model, energy dissipation through frictional sliding may not be sufficient to reach a steady-state solution. Additional dissipation is achieved by small amounts of viscous damping. The forces generated at a contact are computed based on the overlap of the bodies at the contact and the stiffness of the springs. The forces from all of the contacts on a single body are summed yielding a resultant force, which is then used to compute the acceleration of the body according to Newton's second law of motion. After the acceleration is determined, new velocity and displacement for the particle are computed using central difference explicit time integration. With the newly computed displacement configuration, the state of deformation at existing contacts is re-evaluated, and the possible creation of new contacts is evaluated, leading to a new cycle of computation.

2.2. Simulation process

The initial state of the DEM sample is created by random deposition under gravity of particles into a shear box. The top plate on the upper shear box applies a vertical stress $\sigma = 49$ kPa. The DEM sample is composed of circular particles having two diameters of 5 and 9 mm whose mixing ratio by area is 3:2, which mimics an assembly of aluminum rods. We had carried out the direct shear tests on 50 mm long aluminum rods with two different diameters of 5 and 9 mm whose mixing ratio is 3:2 by weight, as shown in Photo 1. To analyze the effects of the frictional force of the shear box in dilative and contractive specimens, two distinct initial states with initial void ratios of $e_0 = 0.196$ and 0.233

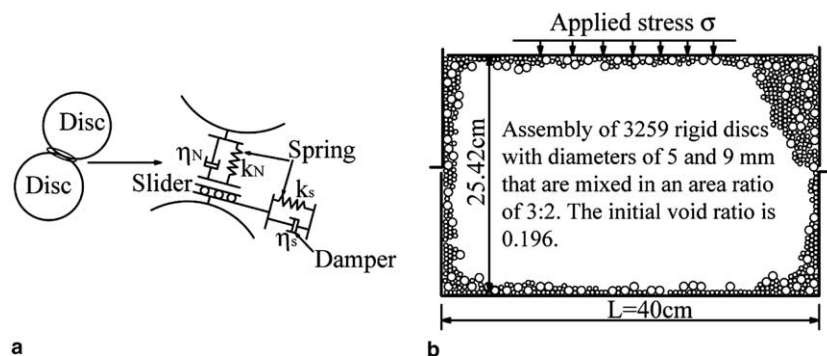


Fig. 2. Simulation of direct shear test: box description and DEM contact model: (a) contact model between particles; (b) dense DEM sample.

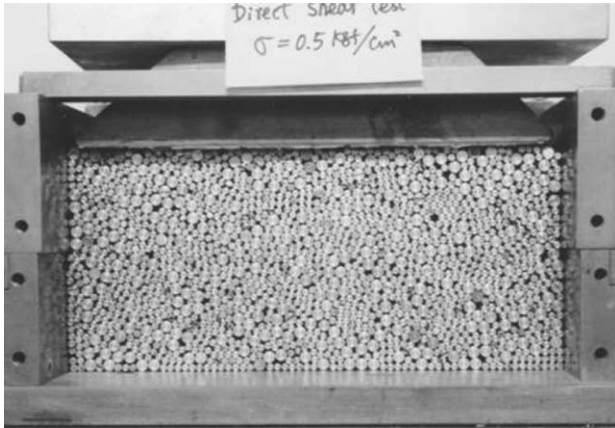


Photo 1. Direct shear test on an assembly of 50 mm long aluminum rods having binary diameters of 5 and 9 mm that is mixed in a weight ratio of 3:2.

are generated. The relatively looser initial state ($e_0 = 0.233$) is obtained by following the above deposition procedure using the particle/particle friction angles $\phi_\mu = 16^\circ$, whereas the relatively denser one ($e_0 = 0.196$) is the result of the same procedure but using $\phi_\mu = 0$. In the latter case, the particle deposition under $\phi_\mu = 0$ is a numerical technique to create a denser sample as used by other researchers, e.g., Thornton [8], Masson and Martinez [9]. The particle/particle friction angle $\phi_\mu = 16^\circ$ is introduced after the deposition under $\phi_\mu = 0$, just before the beginning of the shear action. The two DEM samples have the same binary diameter particles of 3259 contained in a shear box with the same width of 40 cm but with different height. The height of the shear box is 25.42 cm for the denser sample (Fig. 2(b)) and 26.21 cm for the looser sample. It should be pointed out that these initial void ratios are uncompara-

Table 1

Input parameters for numerical simulation by DEM

	Particle/particle	Particle/wall
Normal stiffness k_n, k'_n (N/m/m)	5.0×10^9	9.0×10^9
Shear stiffness k_s, k'_s (N/m/m)	1.5×10^8	3.0×10^8
Normal damping η_n, η'_n (N s/m/m)	5.56×10^4	7.8×10^4
Shear damping η_s, η'_s (N s/m/m)	0.99×10^4	1.4×10^4
Interparticle friction angle ϕ_μ, ϕ'_μ ($^\circ$)	16	16
Density of particles ρ (kg/m ³)	2700	
Time increment Δt (s)	5×10^{-7}	

ble to real soils but comparable to aluminum rods. As shown in Fig. 1, in the conventional direct shear test, the upper shear box is usually constricted vertically with a clasp to balance the possible rotation moment of the upper shear box and is attached horizontally by a bearing ring to measure the shear force. As a result, the upper shear box is almost stationary during the shear process. Thus, in our simulation, the upper shear box is fixed in both vertical and horizontal directions. The material is sheared by moving the lower shear box horizontally at a constant speed of 1 mm/s under the application of a constant vertical stress $\sigma = 49$ kPa on the top plate.

The input parameters used in our simulation are summarized in Table 1, which correspond to those of the aluminum material. The stiffness (k_n, k_s) and damping (η_n, η_s) in Table 1 were determined based on the contact theory of two elastic discs by considering the stress level possibly applied on the granular sample. The particle/particle friction coefficient was obtained from frictional tests on aluminum rods. The time step Δt was chosen to be 1/10 times the critical time step Δt_c in order to maintain a quasi-static state during the calculation, where $\Delta t_c = 2\sqrt{m/k}$ is based on the single degree-of-freedom

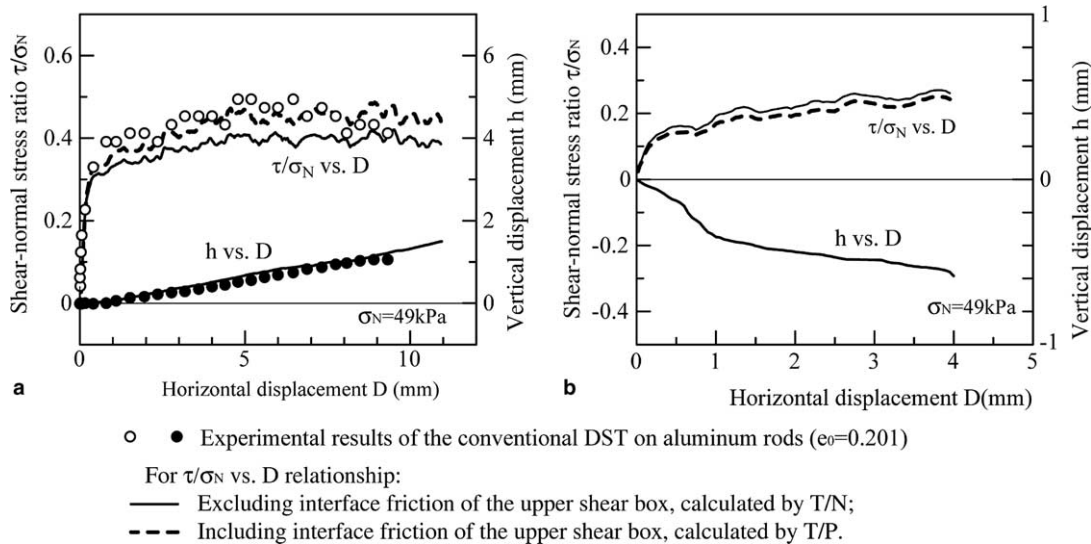


Fig. 3. Numerically simulated evolution of shear-to-normal stress ratio and volume change for the conventional direct shear tests where the upper shear box is fixed: (a) dense DEM sample; (b) loose DEM sample.

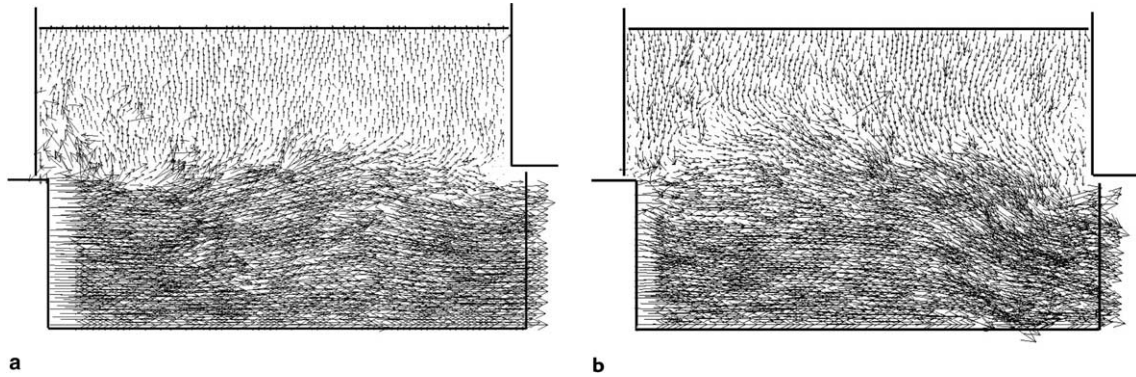


Fig. 4. Particle instantaneous velocity field: (a) dense sample; (b) loose sample.

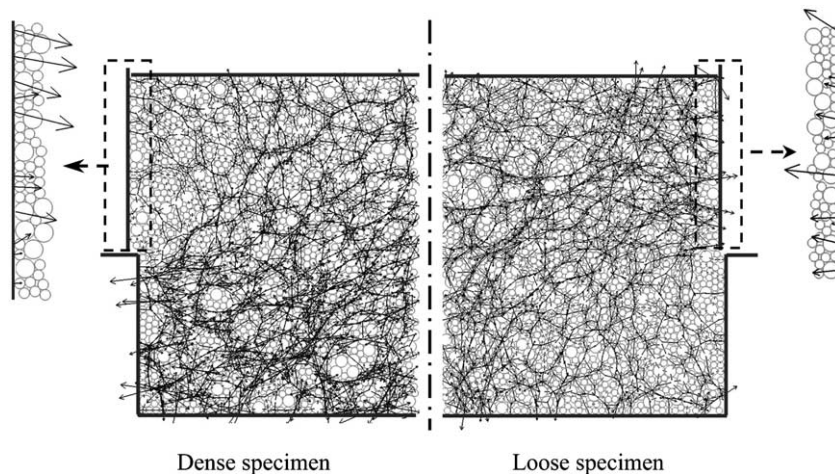


Fig. 5. Particle-particle and particle-wall contact forces network (left: dense sample; right: loose sample).

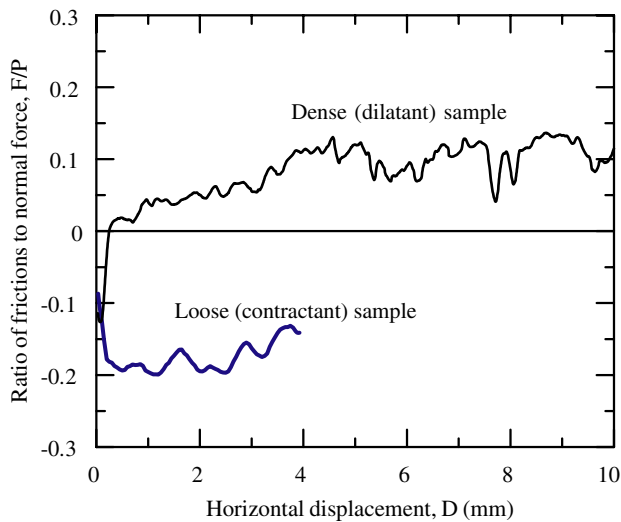


Fig. 6. Evolution of the internal surface friction of the upper shear box in the conventional direct shear test normalized by the applied normal force.

system of a mass m connected to ground by a spring of stiffness k . Yamamoto (1995) [7] and Liu (1999) [10] used the same parameters to simulate a biaxial compression test and a simple shear test on an assembly of aluminum rods with diameters of 5 and 9 mm and a mixing ratio of 3:2 by weight, respectively. The simulated results in terms of macroscopic behavior agreed very well with the experimental ones of the corresponding tests.

2.3. Simulation results

The simulation results in terms of macroscopic behavior are presented for the two initial densities in Fig. 3. The macroscopic shear to normal stress ratio τ/σ is calculated in two ways: T/N and T/P , where T = the shear force on the split plane (shear plane), N = the normal force on the split plane, and P = the externally applied normal force on the top plate, usually recorded in the direct shear test. T and N are deduced from the static equilibrium of the lower half sample by computing the resultant of the horizontal and vertical forces acting on its boundaries (vertical walls and

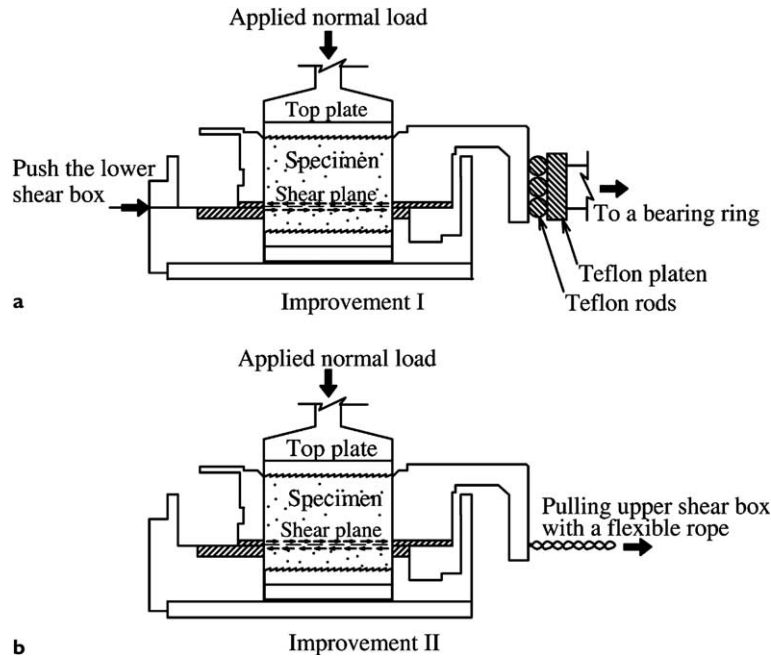


Fig. 7. Improvements for the conventional direct shear test to minimize the interface frictions: (a) using low friction materials of Teflon rods and Teflon platen; (b) pulling the upper shear box with a flexible rope (wire).

bottom plate), respectively. Apparently, T/N is the true stress ratio on the shear plane excluding the effect of the frictional forces of the upper shear box. On the other hand, T/P is the stress ratio equivalent to the value measured from the usual tests involving the frictional forces of the upper shear box. The vertical displacement h is obtained from the vertical displacement of the top plate, representing the overall volume change. The dense sample (Fig. 3(a)) exhibits a very stiff response at the beginning of shearing. As a typical response of dense assemblies, the volume increase observed during shear

characterizes a dilative behavior. Shearing of the loose sample (Fig. 3(b)) is produced with a shear stress increase rate smaller than for the dense one, which clearly leads to a softer macro-shear modulus. The volume change of the loose sample corresponds to a contractive behavior. Thus, these simulations provide macroscopic behaviors that are representative of loose and dense granular materials. Moreover, it can be seen that the stress ratio τ/σ calculated by T/N is smaller than that calculated by T/P for the dense sample and vice versa for the loose sample, which correspond to the experimental fact that the shear strength measured by the conventional direct shear test is overestimated for a dilative specimen and underestimated for a contractive specimen. The experimental results of the conventional DST on the aluminum rods ($e_0 = 0.201$) in accordance with Photo 1 are given together in Fig. 3(a). As the conventional DST involves the influence of the interface frictional force of the upper shear box, the agreement of the experimental stress ratio τ/σ with the calculated one by T/P in Fig. 3(a) illustrates the reasonability of our DEM calculation results.

The particle instantaneous velocity field gives a view of the shear flow within the granular material specimen (Fig. 4). It can be observed within the lower shear box that, both for the dense and for the loose samples, most particles are subject to a block-like motion with the imposed horizontal velocity. The main difference between the velocity fields of the dense and loose samples occurs in the upper shear box. Within the dense sample (Fig. 4(a)), particles are driven by an upward motion corresponding to sample dilation, whereas within the loose

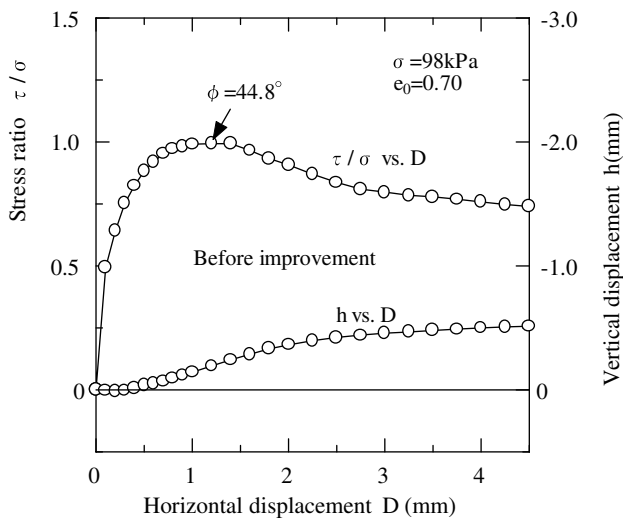


Fig. 8. Laboratory test on Toyoura sand using the conventional direct shear test apparatus as illustrated in Fig. 1.

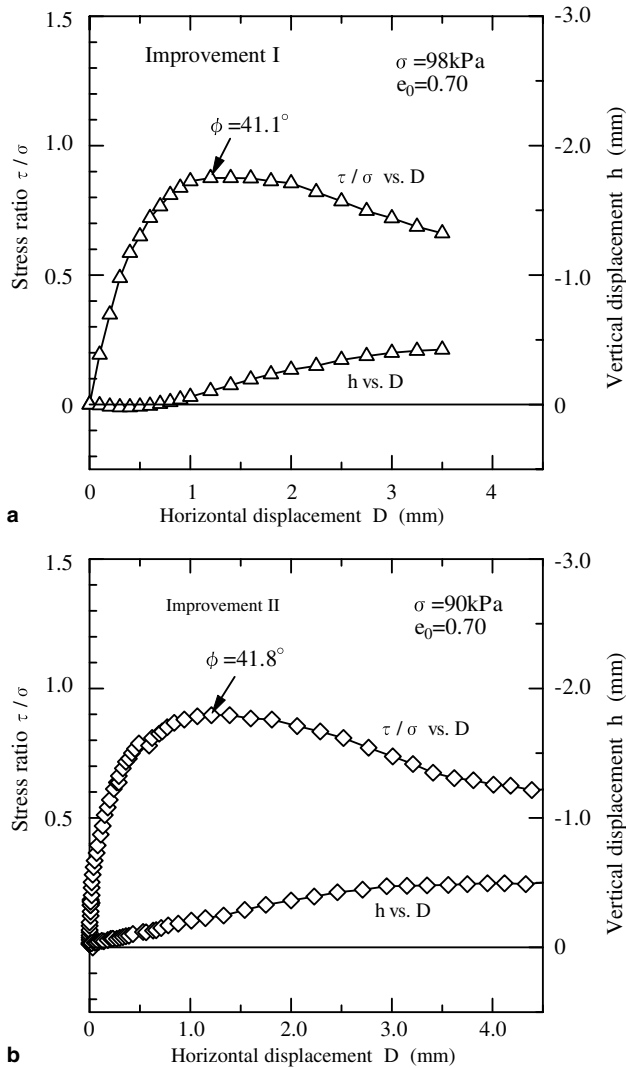


Fig. 9. Laboratory tests on Toyoura sand using the improved direct shear test apparatus corresponding to Fig. 7: (a) using low friction materials of Teflon rods and Teflon platen; (b) pulling the upper shear box with a flexible rope.

sample (Fig. 4(b)), particle motion velocities are downward corresponding to sample contraction.

Fig. 5 shows the contact force networks roughly corresponding to the maximum shear stress: the left side for the dense sample at the shear displacement $D = 7$ mm and the right side for the loose sample at the shear displacement $D = 4$ mm. The force transmissions between the vertical walls of the upper shear box and the boundary particles are enlarged in Fig. 5. Summations of the vertical components of these boundary contact forces yield the frictional forces, denoted by F , between the internal surface of the upper shear box and the sample. Clearly, the orientations of the main boundary contact forces are downward for the dense sample and upward for the loose sample. The evolutions of the ratios of the frictional force F to the externally applied normal force P during the shear process are given in Fig. 6 for

both the dense and loose samples, where the positive value means the same orientations of F and P (downward) and the negative value means the opposite orientations of F and P . It can be seen that shearing of the loose sample produces an upward frictional force F ; whereas for the dense sample, the frictional force F is upward just at the beginning of the shearing where the sample is compressed and then turns to be downward when the sample dilates. Due to the frictional force F , the real normal force N on the shear plane is larger than the externally applied normal force P for the dense sample and vice versa for the loose sample. This explains why the shear strength measured in the conventional direct shear test, determined by T/P , is higher than the true value (T/N) for a dilative sample and vice versa for a contractive sample.

3. Improvements for conventional direct shear test devices

3.1. Improvements and experimental validations

The above discrete modeling gives us a better understanding of the influences of the shear box frictional force F on the shear strength measured in the conventional direct shear test. These influences can be minimized or even eliminated if the upper shear box is allowed to move freely in the vertical direction. This may be achieved using the following two ways. One way is to add smooth materials such as Teflon rods and Teflon plate (the friction coefficient of Teflon material is about 0.02) at the point where the upper shear box contacts the bearing ring that measures the shear force, as shown in Fig. 7(a), abbreviated as Improvement I. The other way is to pull the upper shear box with a flexible rope or chain, as shown in Fig. 7(b), abbreviated as Improvement II. In the latter case, the lower shear box is fixed and the shear force is measured with a load cell that is connected to the rope or chain. To limit the tilt of the upper shear box, the rope or wire should be attached close to the shear plane. An additional requirement for each of these two improvements is that the top plate (loading plate) must be positioned above the rim of the upper shear box in order to prevent it from jamming within the upper shear box in case of the inclination of either the upper shear box or the top plate during the shear.

The above Improvements I and II for the conventional direct shear test device were validated through the tests on Toyoura sand ($D_{50} = 0.2$ mm) with an initial void ratio e_0 of 0.7. The round sample has a diameter of 60 mm and a height of about 20 mm. The applied vertical (normal) stress $\sigma = 98$ or 90 kPa. The test results are presented in Figs. 8 and 9 in terms of the evolutions of the ratio of the measured shear stress τ on the horizontal split plane (shear plane) to the external vertical stress σ

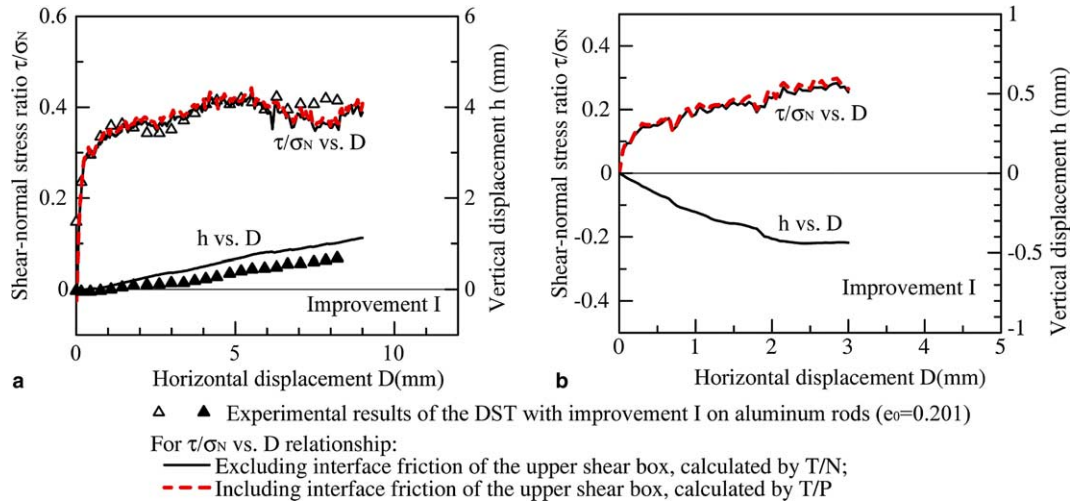


Fig. 10. Numerically simulated evolution of shear-to-normal stress ratio and volume change when the motion of the upper shear box is free in the vertical direction: (a) dense DEM sample; (b) loose DEM sample.

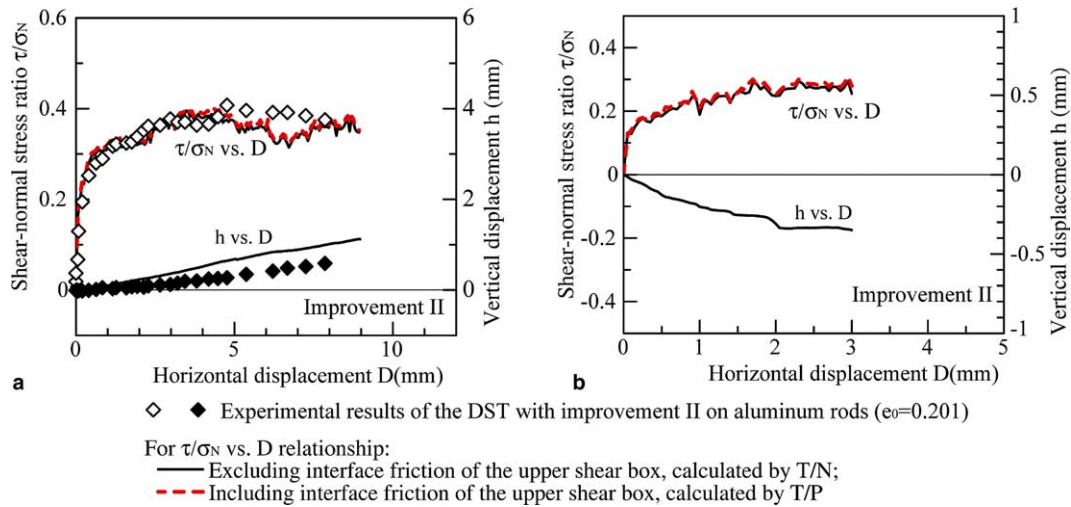


Fig. 11. Numerically simulated evolution of shear-to-normal stress ratio and volume change modeling the pull of the upper shear box: (a) dense DEM sample; (b) loose DEM sample.

as well as the vertical displacement h of the top plate with the horizontal displacement D . Without any improvements for the DST device (the conventional DST), the internal angle of friction ϕ measured from the tests is 44.8° (Fig. 8). As shown in Fig. 9, with the improvements I and II, the measured internal angle of friction ϕ decreases to be 41.1° and 41.8° , respectively. On the other hand, the internal angle of friction of Toyoura sand with the same initial void ratio e_0 was measured to be about 40° by the triaxial compression test [11]. Obviously, the internal angles of friction of Toyoura sand obtained in the cases of improvements I and II are close to the one measured by the triaxial compression test. In a general, the shear strength measured by the direct shear test does not agree completely with that measured by the triaxial compression test because

in the direct shear test there is a predetermined failure plane and shear deformation is of plane strain [12]. But, the similarity justifies the effectiveness of both the improvements I and II to reduce the interface friction of the shear box. These test results further indicate that owing to the influence of the frictional force of the upper shear box, a higher internal angle of friction was measured in the conventional direct shear test on dilative sample without any improvements.

3.2. Discrete simulations for the improved direct shear tests

After the improvement I, the vertical motion of the upper shear box becomes relatively smooth because the rolling friction of Teflon rods is very small. So, in

the discrete simulation for improvement I, the upper shear box is allowed to move freely in the vertical direction. The other simulation conditions are identical with those in the simulation for the conventional direct shear test. In the simulation for improvement II, the lower shear box is fixed in both the vertical and the horizontal directions, and the upper shear box is free in the vertical direction, too. Shearing of the sample is produced by moving the upper shear box together with the top plate horizontally.

The simulation results in terms of the macroscopic behaviors for the improvements I and II are presented in Figs. 10 and 11, respectively. It can be seen that the evolutions of the shear-normal stress ratios determined by T/N agree quite well with the ones determined by T/P for both the improvements I and II, irrespective of the dense and loose samples. This indicates that after the improvements I and II, the frictional force F between the internal surface of the upper shear box and the sample is greatly reduced, so that the normal force N acting on the shear plane is quite close to the normal force P externally applied on the top plate. The above simulation results have been validated in Figs. 10(a) and 11(a) through the comparison with the experimental results of the improved DSTs on the aluminum rods ($e_0 = 0.201$, Photo 1).

For the dense sample, the ratio of the frictional force F to the external normal force P after the improvements I and II as they developed throughout the tests are shown in Fig. 12. As illustrated in Fig. 12, although the ratios F/P fluctuate slightly during the shearing process, the fluctuation amplitudes are very small and their average values are equal to zero both in the cases of the improvements I and II, which are quite different from the observations in the simulation for the standard direct shear box test on the dense sample (Fig. 6). A similar result is obtained for the simulated tests on the loose sample.

3.3. Discussions

In direct shear test, the accurate measurement for shear strengths is controlled by the accurate measurement of the normal force N acting on the horizontal split plane (shear plane). However, in usual experiments, one can only measure the normal force P externally applied on the loading plate, which does not agree with the normal force N due to the influence of the frictional force F between the internal surface of the upper shear box and the sample. The above stated improvements I and II provide two possible ways to reduce the influences of the interface frictional force F , resulting in the good

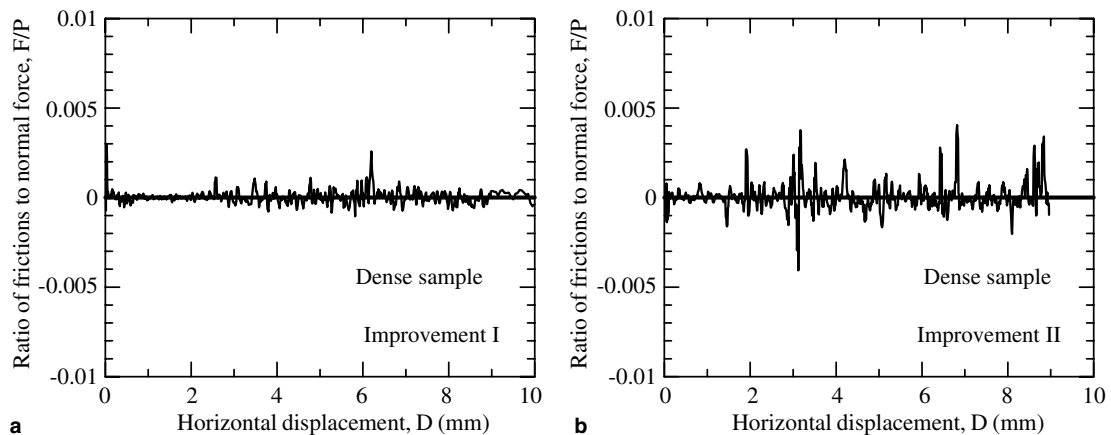


Fig. 12. Evolution of the upper shear box frictions normalized by the applied normal force in the improved direct shear tests on the dense sample: (a) improvement I; (b) improvement II.

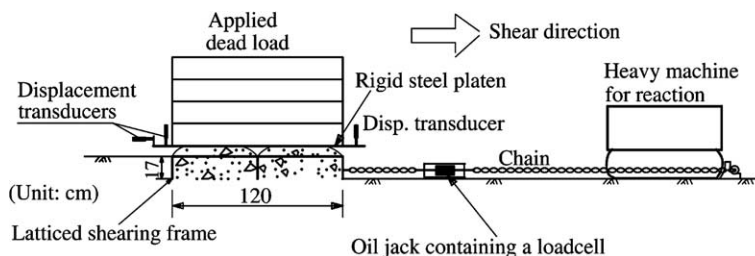


Fig. 13. Schematic of a newly developed in situ direct shear test.

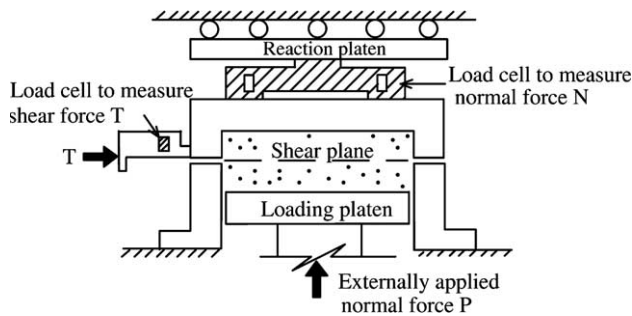


Fig. 14. Schematic of direct shear test device standardized by Japanese Geotechnical Society (JGS) in 1997.

agreement of P and N . Based on the same idea as the improvement II, a new in-situ direct shear testing method has been developed and applied to determine with high accuracy the shear strengths of soils ranging from coarse-grained rockfill materials to fine-grained clay [11,13]. Fig. 13 shows the schematic view of the new in-situ direct shear test. In this new direct shear test, a latticed shearing frame, equivalent to the upper shear box in the conventional direct shear test, is pulled with a flexible chain or rope while a dead load is applied to the sample. The latticed shearing frame is directly embedded into the testing ground.

In the above discrete simulations, the normal force N on the shear plane is deduced from the static equilibrium of the lower half sample by computing the resultant of the vertical forces acting on its boundaries (vertical walls and bottom plate of the lower shear box). This suggests that the normal force N can be accurately measured at the opposite side of the loading plate based on the static force equilibrium in the vertical direction. The Japanese Geotechnical Society (1997) [14] made a standardization for the direct shear test to measure the normal force N by the load cell setting between the reaction plate and the shear box, as shown in Fig. 14.

4. Concluding remarks

Discrete simulations of direct shear tests on loose and dense samples of a granular material were performed using the distinct element method. The simulation results give us a better understanding of the influences of the frictional force F between the internal surface of the upper shear box and the sample on the shear strengths. In the conventional direct shear test, since the lower shear box is pushed horizontally while the up/downward movement of the upper shear box is restrained, the frictional force F acting on the sample is downward for the dense sample (dilative sample)

and upward for the loose sample (contractive sample), causing the shear strength calculated from the externally applied normal force to be an overestimate for the dense sample and an underestimate for the loose sample. The influences of the frictional force F on the shear strength measured in the direct shear test can be minimized, or even eliminated, if the upper shear box is allowed to move freely in the vertical direction or the normal force is measured at the opposite side of the loading plate. Two ways of allowing the upper shear box move freely were presented in this paper. Both experimental and the discrete simulation results have verified the effectiveness of these improvements.

References

- [1] Taylor DW. Fundamentals of soil mechanics. New York: Wiley; 1948.
- [2] Skempton AW, Bishop AW. The measurement of the shear strength of soils. *Géotechnique* 1950;2:98.
- [3] Takada N, Oshima A, Sakamoto A. Effect of specimen thickness of split box shear test under constant pressure condition (Part 1). In: Proceedings of the 31th Japan national conference on geotechnical engineering; 1996. p. 669–70 [in Japanese].
- [4] Sumi T, Oshima A, Takada N, Fukami T. Effect of specimen thickness of split box shear test under constant pressure condition (Part 2). In: Proceedings of the 52th annual conference of the Japan society of civil engineers, vol. III-A30; 1997. p. 60–1 [in Japanese].
- [5] Cundall PA. A computer model for simulating progressive, large scale movements in blocky rock systems. *Proc Int Symp Soc Rock Mech* 1971;2:129–36.
- [6] Cundall PA, Strack ODL. A discrete numerical model for granular assemblies. *Géotechnique* 1979;29(1):47–65.
- [7] Yamamoto S. Fundamental study on mechanical behavior of granular materials by DEM. Dr. Eng. Dissertation, Nagoya Institute of Technology, Japan; 1995 [in Japanese].
- [8] Thornton C. Numerical simulations of deviatoric shear deformation of granular media. *Geotechnique* 2000;50(1):43–53.
- [9] Masson S, Martinez J. Micromechanical analysis of the shear behavior of a granular material. *J Eng Mech, ASCE* 2001;127(10):1007–16.
- [10] Liu SH. Development of a new direct shear test and its application to the problems of slope stability and bearing capacity. Dr. Eng. Dissertation, Nagoya Institute of Technology, Japan; 1999.
- [11] Matsuoka H, Liu SH. Simplified direct shear box test on granular materials and its application to rockfill materials. *Soils Found* 1998;38(4):275–84.
- [12] Takeda N. Mikasa's direct shear apparatus, test procedures and results. *Geotechn Test J, GTJODJ, ASTM* 1993;16(3):314–22.
- [13] Matsuoka H, Liu SH, Sun DA, Nishikata U. Development of a new in-situ direct shear test. *Geotechn Test J, GTJODJ, ASTM* 2001;24(1):99–109.
- [14] The Japanese Geotechnical Society. Method for consolidated constant pressure direct shear box test on soils. *Tsuchi-to-Kiso, JSSMFE*, 1997;45(1):70–4 [in Japanese].